Case Studies in Construction Materials 17 (2022) e01198

Contents lists available at ScienceDirect

Case Studies in Construction Materials

journal homepage: www.elsevier.com/locate/cscm

Case study

An experimental research on reinforced concrete deep beams fully wrapped with fiber reinforced polymers against shear

Hasan Cem Akkaya [a,*], Cem Aydemir [b], Guray Arslan [a]

[a] Department of Civil Engineering, Yildiz Technical University, Istanbul, Turkey
[b] Department of Civil Engineering, Istanbul Aydin University, Istanbul, Turkey

ARTICLE INFO

Keywords:
Deep beams
Shear behavior
Fiber reinforced polymer
Fully wrapped
The shear span-depth ratio
Carbon

ABSTRACT

This paper presents a comprehensive experimental study to investigate the shear behavior of reinforced concrete (RC) deep beams fully wrapped with fiber reinforced polymer (FRP) strips. A total of eighteen deep beams were tested and the test results were evaluated. The test parameters were the shear span-to-effective depth ratio, the number of FRP layers, the clear spacing of FRP strips and the type of FRP. According to the experimental results, as the shear span-to-effective depth ratio increased, the rate of increase in the shear capacity decreased. On the other hand, the rate of increase in the deflection capacity increased with the shear span-to-effective depth ratio. It was observed that the steel plates used at the supports and loading point affected the contribution of FRP strips and the shear behavior of beams. Moreover, increasing the number of FRP layers, reducing the clear spacing of FRP strips or using glass FRP strips enhanced the shear and deflection capacities of beams. A comparative study was also conducted based on the experimental results. Comparisons between the experimental results of this study and the predictions obtained from a total of twelve models consisting of those given by the codes and those proposed by various researchers. The model superior to the others statistically is the one proposed by the German code.

1. Introduction

Reinforced concrete (RC) beams having a relatively high ratio of height to depth may be referred to as deep beams. In general, a RC beam with a shear span-to-effective depth ratio (a_v/d) equal to or less than 2 is considered as a deep beam [1]. According to ACI318–19 [2], a beam is defined as deep if the ratio of clear span length from one support face to the other (l_e) to beam height is less than 4. Eurocode 2 [3] defines a deep beam as a beam with the ratio of span length from one support center to the other (L_e) to beam height being less than 3. The structural behavior of RC deep beams differs from the structural behavior of slender beams (a_v/d>2) as they undergo nonlinear deformations along the beam depth. In addition, RC deep beams have high shear capacities and a relatively simple load transfer mechanism referred to as strut and tie (STM) mechanism [4–8]. In many high-rise buildings, they were used as shear walls and transfer girders. Therefore, the design, maintenance, repair and retrofit of these beams are of great importance.

Service lives of RC deep beams decrease due to many reasons such as corrosion, fatigue, environmental factors, aging of concrete, changes in loadings and the purpose of use [9]. In order to improve the service lives and load capacities of RC deep beams, fiber reinforced polymers (FRPs) has been attractive strengthening material since three decades because of their advantages such as

* Corresponding author.
E-mail address: h.cemakkaya@gmail.com (H.C. Akkaya).

https://doi.org/10.1016/j.cscm.2022.e01198
Received 4 February 2022; Received in revised form 5 May 2022; Accepted 25 May 2022
Available online 27 May 2022

Nomenclature

A_{fv}	Area of FRP shear reinforcement (mm2)
a_t	factor of reduction of FRP effectiveness
b_w	width of beam (mm)
C_E	Environmental reduction factor
D_f	stress distribution factor
d	effective depth of beam (mm)
d_{fv}	Effective depth of FRP shear reinforcement (mm)
E_f	Tensile modulus of elasticity of FRP (MPa)
FC	confident factor
f_{cm}	mean value of concrete compressive strength (MPa)
f_{ctm}	mean value of concrete tensile strength (MPa)
$f_{fd,max}$	maximum design stress in FRP (MPa)
f_{fe}	Effective stress in FRP (MPa)
f_{fu}	ultimate FRP tensile strength (MPa)
f_{fd}	FRP debonding stress (MPa)
h_{fe}	effective height of the bonded reinforcement (mm)
h_w	height of beam's web (mm)
k_R	geometrical coefficient depending on rc
k_b	covering factor
k_G	corrective factor (mm)
L_e	effective bond length (mm)
P_{cr}	the initial shear crack load (kN)
P_u	maximum load (kN)
n	number of FRP layers
n_{cs}	coefficient
R	reduction factor
r_c	radius at beam corners (mm)
s_f	center to center spacing of FRP strips (mm)
s_u	ultimate FRP-support slip (mm)
t_f	thickness of FRP strips (mm)
V_f	Predicted shear strength contribution by FRP (kN)
V_{fe}	Shear strength contribution by FRP (kN)
v_f	Nominal predicted shear strength contribution by FRP (MPa)
v_{fe}	Nominal shear strength contribution by FRP (MPa)
w_f	width of FRP strips (mm)
z	inner lever arm (mm)
z_t	coordinate of upper edge of effective FRP on sides
z_b	coordinate of lower edge of effective FRP on sides
α	Angle of FRP sheet to longitudinal axis of member
Γ_{rd}	design value of the specific fracture energy (N/mm)
ΔP_u	the increase rate of shear capacity (%)
$\Delta\delta_u$	the increase rate of deflection capacity (%)
δ_u	maximum deflection at maximum load
ε_{fe}	Effective strain in FRP shear reinforcement (mm/mm)
ε_{fu}	design rupture strain in FRP shear reinforcement (mm/mm)
$\varepsilon_{fk,e}$	characteristic value of effective FRP strain (mm/mm)
ζ	coefficient
θ°	angle of main shear crack
ρ_f	FRP shear reinforcement ratio
ρ_v	vertical shear reinforcement ratio
ρ_h	horizontal shear reinforcement ratio
ρ_s	tensile steel reinforcement ratio
ρ'_s	compression steel reinforcement ratio
ϕ_r	reduction factor due to local stress in corners

lightweight, high strength, high stiffness, low density, non-corrosiveness, fatigue resistance, easy to be stored and applied in any shape [10,11]. Even though carbon FRP (CFRP) is the mostly used one, glass FRP (GFRP) has begun to be used widely. Additionally, FRP made of aramid and basalt have also been used [12,13]. FRP has been used as a strengthening material in the form of strips, sheets, bars, ropes or grids. Since steel is vulnerable against corrosion, the use of FRP bars instead of steel bars has attracted the attention of researchers. For example, Farghaly and Benmokrane [14] conducted an experimental and analytical study using GFRP and CFRP bars as longitudinal tensile reinforcement. In addition, Ahmed et al. [15] carried out an experimental and analytical study on bridge girders with CFRP stirrups instead of steel stirrups and showed that the contribution of the FRP stirrups calculated using JSCE (1997) [16] code was underestimated. FRP can be applied to structural elements such as beams, columns and beam-column joints in three different techniques known as externally bonding (EB), near surface mounting (NSM) and embedding through-section (ETS) [17]. The ETS technique is better than the other two techniques in terms of workmanship, avoiding premature debonding and fire resistance. It is applied by placing FRP bars into the core concrete with adhesive epoxy [18]. Sogut et al. [19] strengthened shear-critical beams by using this technique. It was observed that the effectiveness of this technique decreased as the shear reinforcement ratio increased. It was also observed that the embedding depth of FRP bars was more effective than the diameter of the hole in the tensile test [20]. As for NSM method, FRP bars are placed into concrete cover of the structural elements. An experimental study involving the application of the NSM technique yielded improvements in the strength and ductility of deep beams [21] and beam-column joints [22,23].

The EB technique has been preferred more than traditional applications such as concrete jacketing and using steel and wood sections. There are three types of schemes used for strengthening against shear, which are fully wrapping (W), U-wrapping (U), and side bonding (S). One of the failure modes encountered in strengthening with FRP is debonding, which occurs mostly in case of RC beams strengthened with U-wrapping or side bonding FRP. Debonding of FRP is a premature failure since the capacity of FRP becomes wasted. To eliminate this disadvantage, researchers conducted experimental studies on U-shaped cementitious mortar jacketing and mechanically anchored U-wrapping scheme [24,25]. In case of RC beams fully wrapped with FRP, the rupture of FRP occurs before the failure of beam indicating a complete use of the capacity of FRP. Therefore, fully wrapping results in a superior performance in terms of the contribution of FRP to the shear capacity of beam [26,27]. The efficiency of FRP depends also on the type of FRP, the shear reinforcement ratio, the tensile reinforcement ratio, a_v/d and the FRP strip ratio [28–33]. In this study, the parameters affecting the efficiency of FRP strips used to strengthen RC deep beams were investigated.

There are many experimental and theoretical studies on the slender beams strengthened with FRP against shear or flexural [34–44]. Grande et al. [45] carried out an experimental and analytical study to investigate the effect of transverse reinforcement on the efficiency of FRP. Three different strengthening schemes (W, U and S) were applied to the slender beams ($a_v/d=3$) using CFRP. It was observed that the efficiency of CFRP decreased as the transverse reinforcement increased. Similarly, the experimental study conducted Karzad et al. [46] showed that the contribution of CFRP decreased as the transverse reinforcement ratio increased and the shear capacity was improved approximately 30% by adding another layer of CFRP on RC slender beams U-wrapped with CFRP. On the other hand, ACI [47] and Fib Codes [61] do not consider the correlation between transverse reinforcement and FRP strips.

Compared to the studies on slender beams, experimental or theoretical studies on RC deep beams strengthened with FRP are scarce. Few studies [48–51] showed that RC deep beams strengthened with FRP improves the behavior in terms of load-carrying capacity, ductility, delay in formation of critical crack and serviceability. Bousselham and Chaallal [52] carried out a comprehensive study on T-beams strengthened with CFRP and showed that (i) the contribution of CFRP to the shear capacity was higher in deep beams than in slender beams, (ii) the contribution of CFRP decreased as the transverse reinforcement ratio increased, and (iii) the shear capacity increased slightly with the number of CFRP layers. On the other hand, the codes ACI 440.2R-02[53], CSA S806–02[54] and Fib-TG9.3 [61] do not consider the effect of parameters such as a_v/d and transverse reinforcement ratio while calculating the shear strength (V_f).

One of the most important parameters affecting the shear behavior of beams is the a_v/d whose effect cannot be fully explained in case of the beams strengthened with externally bonded FRP since there exist a limited amount of studies examining the effect of a_v/d on the behavior of beams strengthened with FRP. Li and Leung [55] carried out an experimental and analytical study on the effect of a_v/d involving RC beams with stirrups strengthened by fully-wrapping them with CFRP. It was observed that the contribution of FRP to the shear capacity was low for lower values of a_v/d and the contribution of FRP to the shear strength (V_f) calculated according to JSCE-2001[56] and FIB-TG9.3–2001[61] was not safe for low a_v/d ($a_v/d=1$). CSA S806–12[66], CNR-DT200–2013 and ACI 440.2R-2008 [47] delivered, on the other hand, overly conservative predictions of V_f. CSA S806–2012 [66] and ACI 440.2R-2008 [47] delivers reliable predictions of V_f for beams U-wrapped with CFRP except those with low a_v/d [57]. Cao et al. [58] conducted an experimental and analytical on RC beams fully wrapped with CFRP and GFRP and concluded that it is necessary to investigate the effect of a_v/d well in order to accurately predict the effectiveness of FRP.

Since GFRP is more economical than CFRP, it has attracted the attention of researchers and various studies on RC deep beams strengthened with GFRP have been recently carried out. Kumari and Nayak [59] showed that using GFRP improved the shear strength and ductility of RC deep beams, and delayed the formation of initial shear crack.

This paper presents an extensive experimental study involving eighteen RC deep beams strengthened with externally bonded FRP strips using the fully wrapping scheme. The test parameters were the shear span-to-effective depth ratio, the number of FRP layers (1 or 2), the clear spacing of FRP strips (50 mm or 100 mm) and the type of FRP (carbon or glass). The experimental results provide important insights on the shear performance and failure mode of the strengthened RC deep beams. Providing data to the literature and contributing to the theoretical studies in the future with test results are the main motives for Authors in this research. Furthermore, a comparative study for evaluating the contribution of FRP strips to the shear strength of RC deep beams was also carried out. The contribution of FRP strips to the shear strength was predicted using the shear models proposed by various codes and researchers [60–71].

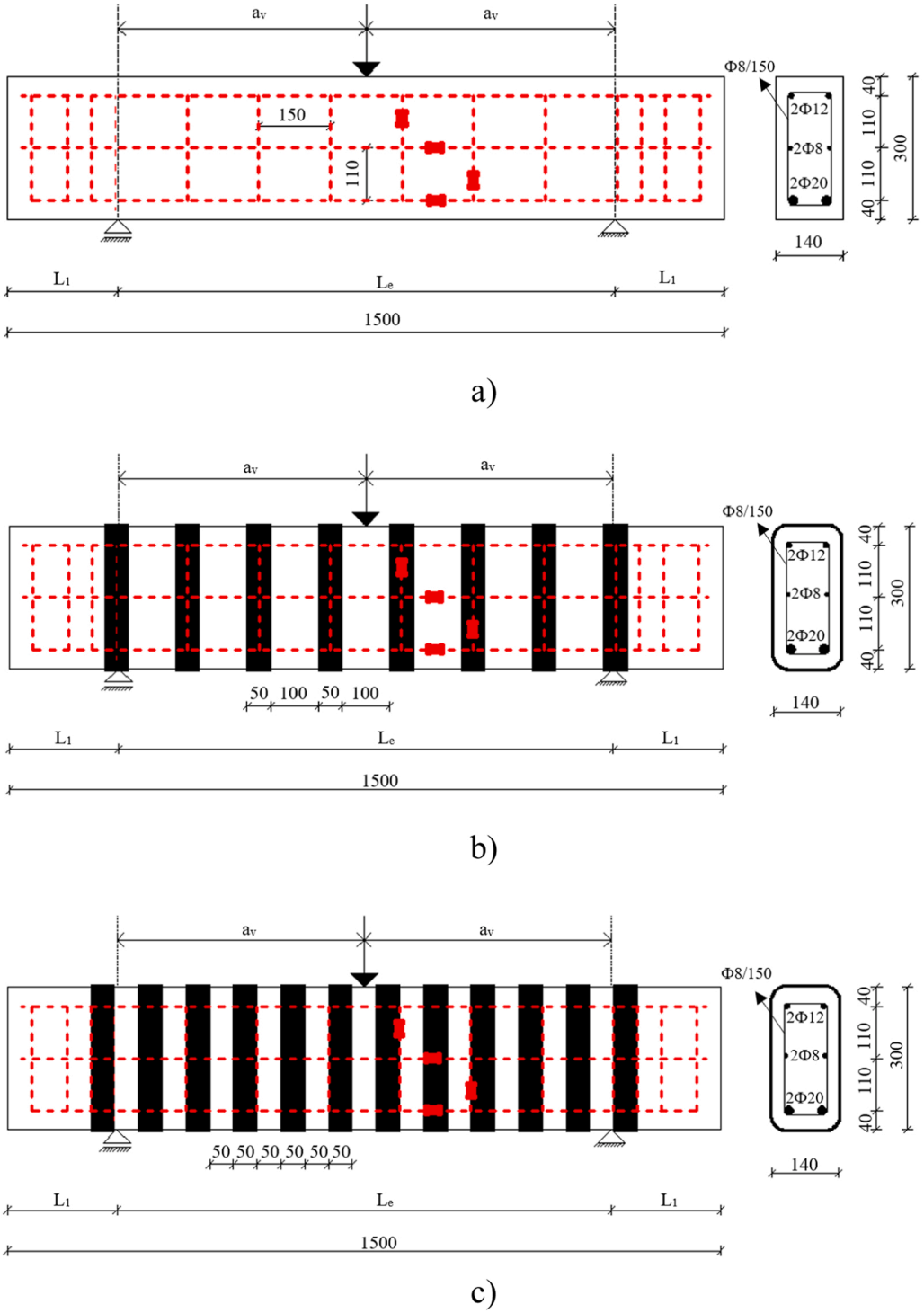

Fig. 1. : Test Specimens; a) Unstrengthened, b) Strengthened with FRP strips having a clear spacing of 100 mm, c) Strengthened with FRP strips having a clear spacing of 50 mm (dimensions in mm).

2. Experimental program

2.1. Test specimens

In total, eighteen RC deep beams with stirrups were constructed. While five of them were reference beams, the other thirteen beams were fully wrapped with FRP strips. As can be seen in Fig. 1, the total length, height, effective depth and width of the beams were 1500 mm, 300 mm, 260 mm and 140 mm, respectively. In order to consider three different a_v/d as 1, 1.5 and 2, the shear spans of the beams were set to 260 mm, 390 mm and 520 mm, respectively. Two bars of 20 mm diameter having a mean yield strength (f_y) of 548 MPa and a mean tensile strength (f_u) of 647 MPa were used as the longitudinal tensile reinforcement, whereas two bars of 12 mm diameter having a mean yield strength of 601 MPa and a mean tensile strength of 695 MPa were used as the longitudinal compression reinforcement. The shear reinforcements were chosen as Ø8/150 ($\rho_v = 0.0048$) in the vertical direction and 2Ø8/110 ($\rho_h = 0.0065$) in the horizontal direction, where the bars had a mean yield strength of 740 MPa and a mean tensile strength of 881 MPa. Both the vertical and horizontal shear reinforcements were selected in accordance with ACI 318–19[2] Section 23.5, in which it is stated that the minimum shear reinforcement ratio in each direction should be at least 0.0025. The elasticity modulus of all reinforcing bars was 200 GPa. Both ends of the tensile bars were bent up 90° to provide adequate anchoring.

Ready-mixed concrete consisted of 350 kg/m^3 of cement, 860 kg/m^3 of sand, 975 kg/m^3 of aggregate with a maximum aggregate diameter of 12 mm, 168 kg/m^3 of water and 4.55 kg/m^3 of super plasticizer admixture was obtained from a local company. Six 150×150×150 mm cubic samples of concrete were taken during casting and kept in the same environmental conditions with the beams that were cured for 28 days. The upper, lower and mean compressive strengths of the cubic samples were 36.05, 32.56 and 35 MPa, respectively, where the standard deviation was calculated as 1.32. Table 1 gives the properties of the tested beams.

2.2. Strengthening scheme and materials

Thirteen RC deep beams were strengthened by wrapping them with unidirectional fibers made of carbon and glass having an elasticity modulus of 255 GPa and 70 GPa, a tensile strength of 4400 MPa and 3500 MPa, and a thickness of 0.34 mm and 0.35 mm, respectively, as reported by the manufacturer. 50 mm wide FRP strips were wrapped around the beams perpendicular their longitudinal axes with a certain spacing along their shear spans. Ten beams were strengthened with CFRP strips, while GFRP was used to strengthen three beams. Fig. 1b and c show the geometrical properties of strengthening scheme.

Prior to the FRP application, all surfaces of the beams were sanded until aggregates were visible and the corners were rounded to avoid stress concentrations and to provide a better bonding between the FRP strips and the beams. Before surface cleaning, 2–3 mm of cover concrete at areas where FRP strips would be placed were removed. After cleaning, all surfaces were coated by an epoxy-based primer. Following a 24 h waiting period, FRP strips were placed in their predetermined locations by means of a mixture of epoxy-based primer and hardener resin in a ratio of 2:1 according to the manufacturer's instructions. The mixture was dispersed homogenously by means of an iron roller. Following the recommendation of manufacturer, beams were cured at least for 28 days under laboratory conditions.

Beams were labeled in such a way that a label starts with either "UDB" indicating an unstrengthened beam or "SDB" indicating a strengthened beam. The letters are followed by a_v/d (1, 1.5 or 2) and then the number "46" referring to vertical and horizontal shear reinforcement ratios ("4" for $\rho_v = 0.0048$ and "6" for $\rho_h = 0.0065$). If it is a reference beam, the label ends with the letter "R". If it is a

Table 1
Properties of test specimens.

Beams	ρ_s	ρ'_s	ρ_v	ρ_h	a_v/d	s_f (mm)	ρ_f	L_{base} (mm)	L_{load} (mm)
UDB1–46-R	0.0173	0.0062	0.0048	0.0065	1	–	–	20	70
UDB1–46-RT	0.0173	0.0062	0.0048	0.0065	1	–	–	100	150
UDB1.5–46-R	0.0173	0.0062	0.0048	0.0065	1.5	–	–	20	70
UDB1.5–46-RT	0.0173	0.0062	0.0048	0.0065	1.5	–	–	100	150
UDB2–46-R	0.0173	0.0062	0.0048	0.0065	2	–	–	20	70
SDB1–46-C1–10	0.0173	0.0062	0.0048	0.0065	1	150	0.0016	20	70
SDB1.5–46-C1–10	0.0173	0.0062	0.0048	0.0065	1.5	150	0.0016	100	150
SDB2–46-C1–10	0.0173	0.0062	0.0048	0.0065	2	150	0.0016	100	150
SDB1–46-C2–10	0.0173	0.0062	0.0048	0.0065	1	150	0.0032	20	70
SDB1–46-C2–10 T	0.0173	0.0062	0.0048	0.0065	1	150	0.0032	100	150
SDB1.5–46-C2–10	0.0173	0.0062	0.0048	0.0065	1.5	150	0.0032	100	150
SDB2–46-C2–10	0.0173	0.0062	0.0048	0.0065	2	150	0.0032	100	150
SDB1–46-C1–5	0.0173	0.0062	0.0048	0.0065	1	100	0.0024	100	150
SDB1.5–46-C1–5	0.0173	0.0062	0.0048	0.0065	1.5	100	0.0024	100	150
SDB2–46-C1–5	0.0173	0.0062	0.0048	0.0065	2	100	0.0024	100	150
SDB1–46-G1–10	0.0173	0.0062	0.0048	0.0065	1	150	0.0017	100	150
SDB1.5–46-G1–10	0.0173	0.0062	0.0048	0.0065	1.5	150	0.0017	100	150
SDB2–46-G1–10	0.0173	0.0062	0.0048	0.0065	2	150	0.0017	100	150

Notes : $\rho_f = 2n_f w_f t_f / b_w s_f; \rho_s = A_s/b_w d; \rho'_s = A'_s/b_w d; \rho_v = A_v/b_w s_v; \rho_h = A_h/b_w s_h$

strengthened beam, the label continues with the type of FRP ("C" or "G") followed by the number of FRP layers ("1" or "2"). The label ends with a number ("5" or "10″) indicating the clear spacing between FRP strips. The letter "T" at the end of a label indicates the use of steel plates at the supports and loading point.

2.3. Test setup and instrumentation

Test specimens were subjected to three-point bending tests by using a 1000 kN capacity displacement-controlled testing machine. A data acquisition system was used to monitor and record experimental data. Linear Variable Displacement Transducers (LVDTs) were used to measure deflections of beams. A total of five strain gauges were installed on shear and longitudinal tensile reinforcements as shown in Fig. 2. The locations were selected in the vicinity of regions likely to be stressed most. Also, cracking patterns were monitored throughout the experiments.

3. Test results

3.1. Behavior of test specimens

The beams at failure state are shown in Fig. 3. UDB1–46-R, SDB1–46-C1–10 and SDB1–46-C2–10 failed by crushing of concrete in the vicinity of loading point. As given in Table 2, the increases in the shear capacities of SDB1–46-C1–10 and SDB1–46-C2–10 with respect to the reference beam UDB1–46-R were 21.60% and 15.58%, respectively. It was observed that increasing the number of FRP layers did not increase the shear capacity significantly. However, as can be seen in Fig. 3, the CFRP strips close to the loading point remained ineffective due to the crushing of concrete, so it was likely that they were not able to contribute to the shear capacity. To delay the crushing of concrete in the vicinity of supports and loading point, 100 × 140 mm and 150 × 140 mm steel plates were placed at the supports and the loading point, respectively, and the beams UDB1–46-RT and SDB1–46-C2–10 T, which were the backups of UDB1–46-R and SDB1–46-C2–10, were tested. It was observed that the increase in the shear capacity of SDB1–46-C2–10 T beam compared to the reference beam UDB1–46-RT was 58.19%. While the failure of SDB1–46-C2–10 T occurred by a diagonal shear crack, a thin diagonal shear crack was observed in UDB1–46-RT. As a result, the width of steel plates played an important role in the contribution of FRP strips to the shear strength. Accordingly, the remaining tests were carried out by using steel plates.

The beams UDB1.5–46-R and UDB2–46-R failed also by the formation of diagonal shear cracks. It is known that the shear capacity decreases with the increasing a_v/d while keeping other properties the same, however it was observed that UBD1.5–46-R had a shear capacity less than UDB2–46-R. A possible reason for this was that the shear crack might have not intersected with any shear reinforcement. Similar to UDB1.5–46-R, the failure of UDB1.5–46-RT was also caused by a diagonal shear crack. The beam UDB1.5–46-RT was used as the reference beam for strengthened beams having an a_v/d of 1.5 in Table 2.

The FRP strips was used to increase the confinement of concrete and to prevent the development of shear cracks. The rupture of FRP strips was not observed in the strengthened beams with a large FRP strip spacing (center-to-center spacing s_f =150 mm) except SDB1.5–46-C1–10 because the shear cracks intersected with the FRP strips in the compression region, and they reached the compression region before local debonding of the FRP strips occurred. Therefore, it is recommended that the center-to-center spacing of the FRP strips should not exceed d/2. As mentioned above, the beam SDB1.5–46-C1–10 failed by shear and the rupture of an FRP strip was observed. The increase in its shear capacity was 19.01%. When the number of FRP layers was increased, that is, the beam SDB1.5–46-C2–10, the failure mode was the same, but no rupture of the FRP strips was observed and the increase in the shear capacity increased to 30.53%. It is to be noted that SDB1.5–46-C2–10 beam had a workmanship defect such that the clear spacing between two neighboring FRP strips should have been 100 mm, but it was approximately 170 mm in the vicinity of the loading point. The shear cracks did not intersect with the FRP strips due to this defect. It was observed that the role of FRP strips to prevent cracks from opening and propagating was not fulfilled completely, but the experimental data was considered in the scope this study for analytical study since such workmanship defects are possible in real life. In both the beams SDB2–46-C1–10 and SDB2–46-C2–10, shear cracks were observed as well as wide flexural cracks. The increases in the shear capacities were 32.98% and 36.22%, respectively. Increasing the number of FRP layers by one showed little improvement in the shear capacity of beams having an a_v/d of 2.

The rupture of the FRP strips occurred in beams with the smaller FRP strip spacing (s_f=100 mm) before the beams reached their load carrying capacities, regardless of the a_v/d. Contrary to the experimental study of Li and Leung [55], the increase in the shear

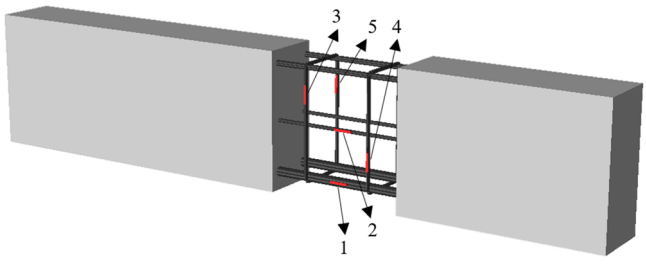

Fig. 2. Locations of strain gauges in perspective view.

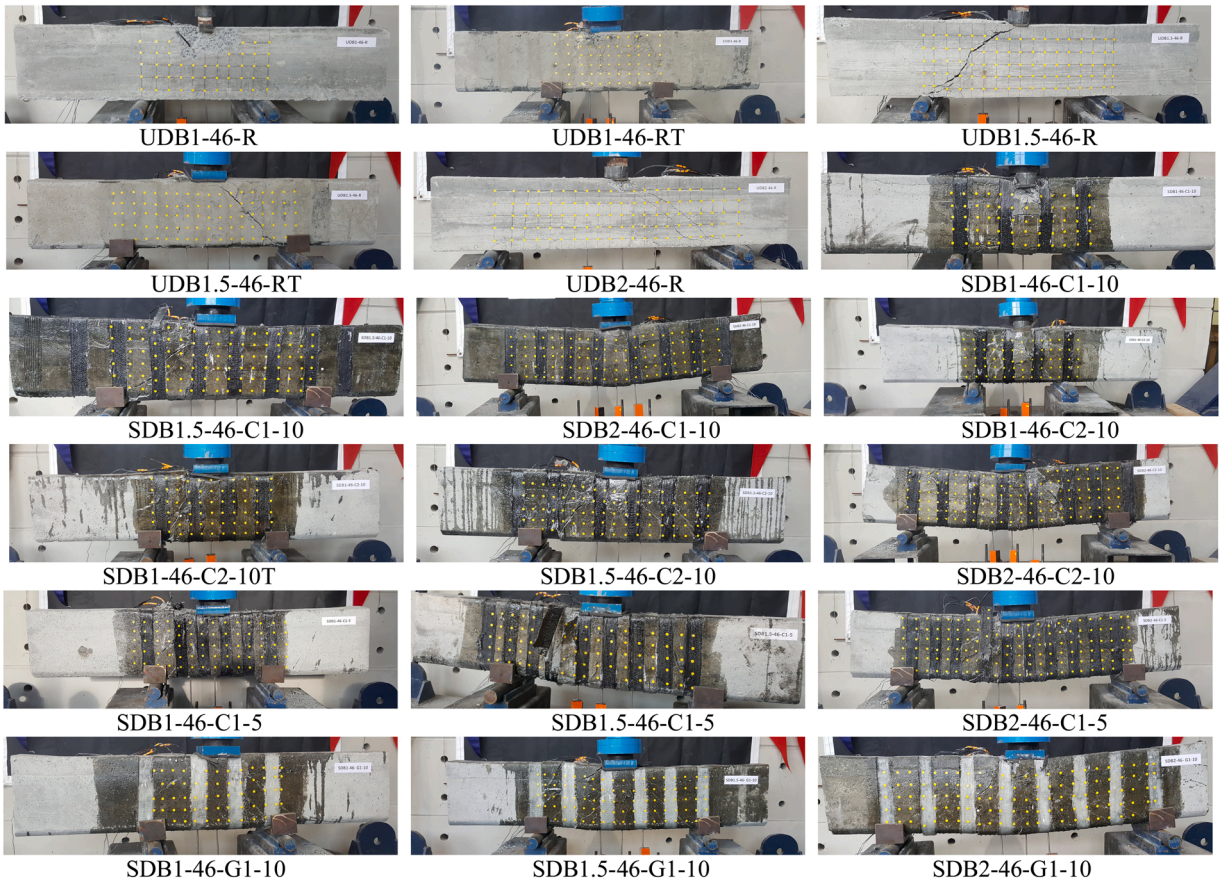

Fig. 3. : Tested beams at failure state.

Table 2
Experimental results.

Beams	P_{cr} (kN)	P_{cr}/P_u (%)	θ^{o}_{shear}	P_u (kN)	δ_u (mm)	ΔP (%)	Δδ (%)	Failure Mode
UDB1–46-R	198.10	61.61	45	321.55	5.30	–	–	Shear-Concrete Crushing
UDB1–46-RT	203.62	59.40	51	342.78	5.44	–	–	Shear-Concrete Crushing
UDB1.5–46-R	136.21	58.69	53	232.08	4.48	–	–	Shear-Diagonal cracking
UDB1.5–46-RT	170.90	57.25	46	298.53	6.08	–	–	Shear-Diagonal cracking
UDB2–46-R	131.49	51.30	38	256.34	6.76	–	–	Shear-Diagonal cracking
SDB1–46-C1–10	188.60	48.23	40	391.01	6.36	21.60	20.00	Shear-Concrete Crushing
SDB1.5–46-C1–10	136.16	38.33	49	355.27	8.94	19.01	47.04	Shear-FRP rupture
SDB2–46-C1–10	111.80	32.80	49	340.89	32.66	32.98	383.14	Shear-Flexural Failure
SDB1–46-C2–10	200.50	54.14	42–52	370.35	7.30	15.18	37.74	Shear-Concrete Crushing
SDB1–46-C2–10 T	222.97	41.12	60	542.25	11.34	58.19	108.46	Shear-Diagonal cracking
SDB1.5–46-C2–10	133.85	34.35	52	389.66	10.38	30.53	70.72	Shear-Diagonal cracking
SDB2–46-C2–10	117.04	33.52	39–54	349.19	30.66	36.22	353.55	Shear-Flexure Failure
SDB1–46-C1–5	222.28	41.42	45	536.63	11.84	56.55	117.65	Shear-FRP rupture
SDB1.5–46-C1–5	130.76	28.22	45	463.33	16.10	55.20	164.80	Shear-FRP rupture
SDB2–46-C1–5	113.32	32.17	36	352.23	28.30	37.41	318.64	Shear-FRP rupture
SDB1–46-G1–10	215.92	47.90	47	450.81	9.10	31.52	67.28	Shear-Diagonal cracking
SDB1.5–46-G1–10	133.41	35.90	41	382.27	10.78	28.05	77.30	Shear-Diagonal cracking
SDB2–46-G1–10	115.97	36.52	26–36	317.53	15.02	23.87	122.19	Shear-Flexural Failure

capacity decreased as the a_v/d increased. It was concluded that increasing the number of FRP layers by one or reducing the spacing of the FRP strips improved the shear and deflection capacities. The beams SDB1–46-G1–10 and SDB1.5–46-G1–10 failed in shear by the formation of diagonal shear cracks. Wide flexural cracks were observed in addition to shear cracks in SDB2–46-G1–10. The increase in the shear capacity decreased as the a_v/d ratio increased also when GFRP was used similar to the beams the smaller FRP strip spacing (s_f=100 mm). GFRP resulted in higher increases in the shear and deflection capacities compared to CFRP in case that a_v/d was 1.5. However, it was the opposite in case of beams having a_v/d of 2.

It can be seen in Table 2 that the deflection capacities of SDB1–46-C1–10 and SDB1–46-C2–10, which were tested without placing steel plates at the supports and loading point, increased by 20.00% and 37.74% compared to the reference beam UDB1–46-R. It was observed that the deflection capacity increased when the number of FRP layers was increased by one. The deflection capacities of beams except SDB2–46-C2–10 increased with the a_v/d.

The first shear crack load decreased as the a_v/d increased in case of all beams involved in this study because the arching effect increases with the decreasing a_v/d and the principal tensile stresses get smaller. It was also observed that the first shear crack loads of the strengthened beams were not significantly different than those of the unstrengthened beams for the same a_v/d. As can be seen in Table 2, the ratio of the first shear crack load to the maximum load by percent decreased with the use of FRP strips or with the increasing a_v/d. The angles of shear cracks were often between 40° and 60°. However, in some beams having an a_v/d of 2, this angle decreased until 26°.

3.2. Load-deflection curves

Fig. 4a depicts the load-deflection curves of UDB beams that exhibited linear elastic behavior initially. When the first shear crack began to appear, the stiffness of the beams started to decrease, and the behavior started to shift from linear to nonlinear. After reaching the failure load, sudden drops in the loads were observed. Fig. 4a shows that UDB beams exhibited nonductile behavior.

Fig. 4(b-d) presents the load-deflection curves of beams classified according to a_v/d. It was observed that both loading and deflection capacities of SDB beams having a_v/d of 1 and 1.5 increased and these beams exhibited nonductile behavior as can be seen in Fig. 4b and c. On the other hand, Fig. 4d shows that SDB beams having an a_v/d of 2 exhibited more ductile behavior compared to the others, which can be attributed to the fact that the arching effect decreases as the a_v/d increases. Even after the first shear crack occurred, the load continued to increase at a steep angle. Moreover, after the beams reached approximately the failure load, it was observed that the load slightly increased, which could be the contribution of FRP to the load carrying and deflection capacities by

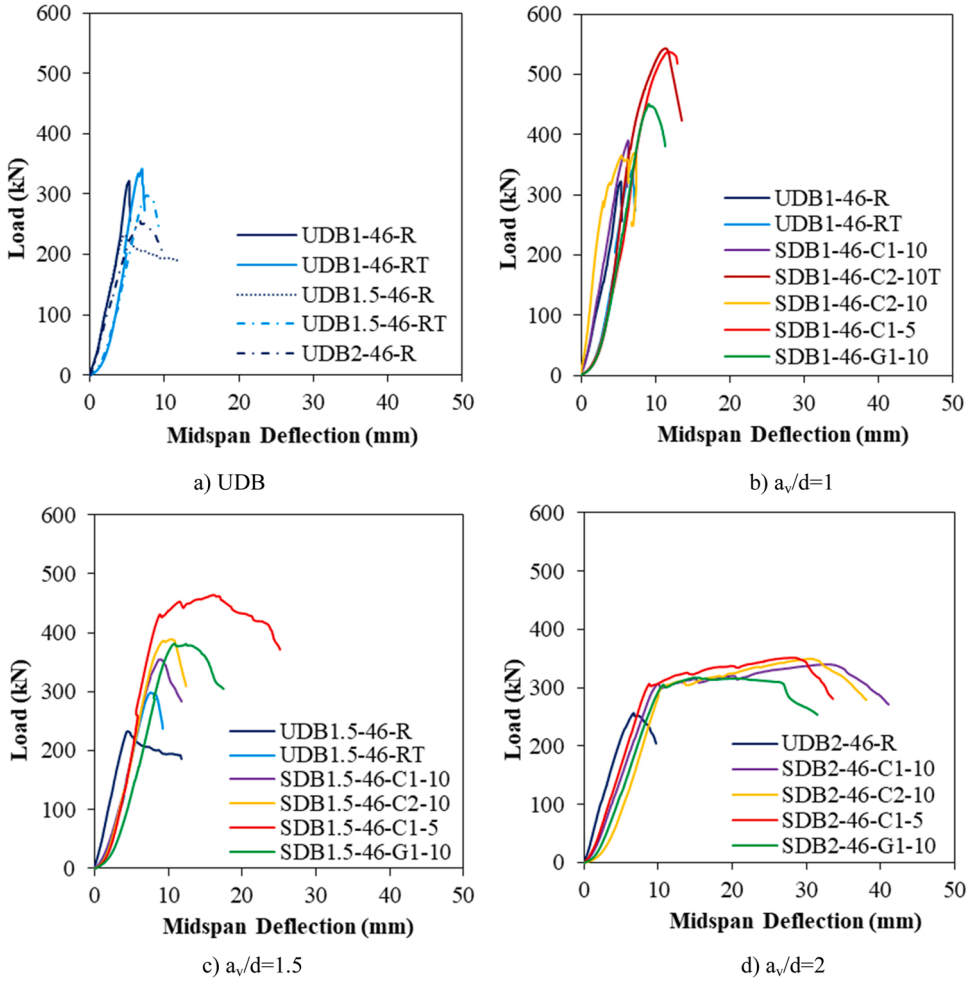

Fig. 4. : Load- deflection curves.

preventing cracks from opening. The most significant test parameter increasing the deflection capacity was to halve the FRP strip spacing in SDB beams having a_v/d of 1 and 1.5. In SDB beams having a_v/d of 2, the most significant test parameter was using a single and double layers of FRP strips, which increased the deflection capacities by 383.14% and 353.55%, when respectively.

3.3. Load-strain curves

Five strain gauges were mounted to the reinforcing bars of each beam, the locations of which are shown in Fig. 2. The strain gauges labeled as "1" and "2" were mounted to the longitudinal tensile reinforcement and the horizontal shear reinforcement, respectively. The strain gauges labeled as "3" and "5" were mounted to the both legs of the vertical shear reinforcement closest to the loading point. The strain gauge labeled as "4" was mounted to the vertical shear reinforcement on the other side of the loading point to the part farther away from the load. Unfortunately, data could not be obtained from some of the strain gauges. The load-strain curves of all beams are given in Figs. 5–9. The yield limits of tensile and shear reinforcements are shown vertically in the Figs. 5–9 with dashed lines.

The first noticeable difference between Figs. 6–9 and Fig. 5 is the horizontal region where the shear load remained constant while the strains increased. This explains the spreading of shear crack while the load remained constant after the initial shear crack formed.

Figs. 6–9 show that shear reinforcements did not take any strain until the first shear crack occurred or the concrete in the vicinity of the supports and loading point was crushed. On the other hand, the strains in tensile reinforcements increased linearly at the initial stages. It can be observed in Fig. 5 that the slope of these linear curves decreased as the a_v/d increased. The strain characteristics in both tensile reinforcement and shear reinforcement were almost similar in SDB beams having a_v/d of 2, regardless of the strengthening parameters. It was observed that CFRP strips resulted in a better behavior than GFRP strips in the scope of preventing the opening and spreading of shear cracks. Reducing the spacing of the FRP strips was the most effective action for this purpose since the strains in SDB1.5–46-C1–5 remained constant despite the increasing load (Fig. 5).

Tensile reinforcement in all beams except SDB1–46-G1–10 yielded. Most of the shear reinforcement in the beams with an a_v/d of 1 did not yield because either the shear crack did not intersect the shear reinforcement or the concrete strut took most of the load. Contrarily, most of the shear reinforcement yielded in the beams with a_v/d of 1.5 and 2. This indicates that the effectiveness of the FRP strips and steel reinforcement varied with the a_v/d of beams. The variation in the strains in the shear reinforcements increased significantly with the formation of shear cracks and rupture or debonding of the FRP strips. As can be seen in Figs. 6–9, the load-strain curves became horizontal after a certain load, and a sudden increase in the strains occurred in case of beams having a_v/d of 1.5 and 2 happened.

4. Comparison of results with predictions

Experimental results (V_{fe}) obtained in this study were compared with the predictions (V_f) obtained from twelve shear models consisting of those given by various codes [60–67] and those proposed by various researchers [68–71]. Table 3 summarizes the considered models. No safety factor was used in calculations. The contribution of the FRP strips to the experimental shear capacity was determined by subtracting the shear capacity of the unstrengthened beam from the shear capacity of the strengthened beam. The comparison of the experimental results with the predictions obtained from the considered models are given in Table 4.

The considered models predict the contribution of the FRP strips to the shear strength not only by considering the FRP strips as transverse shear reinforcement independent of concrete and steel reinforcement, but also assuming that all shear cracks intersect with the FRP strips. However, it is too optimistic to assume that all shear cracks intersect with the FRP strips. As observed in this study, the shear cracks may not intersect with the FRP strips due to a steeper angle of the shear crack, especially in case of beams having relatively low a_v/d. In addition, Chen and Teng [70] reported that the FRP strips cannot provide maximum benefit together with transverse reinforcement and they affect each other. Furthermore, the contribution of the FRP strips to the shear strength depends on many

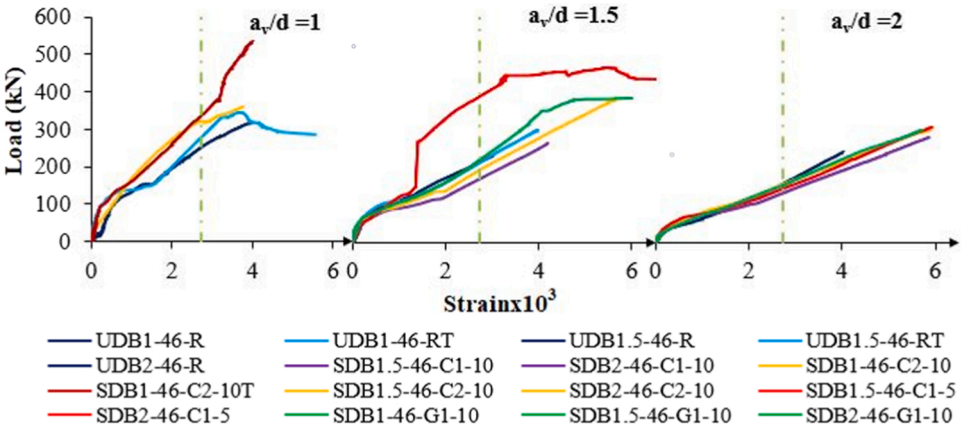

Fig. 5. : Load-strain curves obtained from the strain gauge "1".

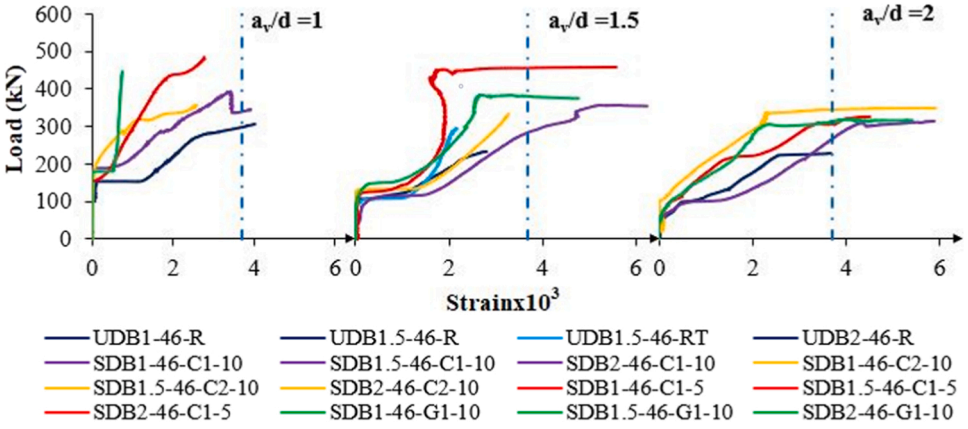

Fig. 6. : Load-strain curves obtained from the strain gauge "2".

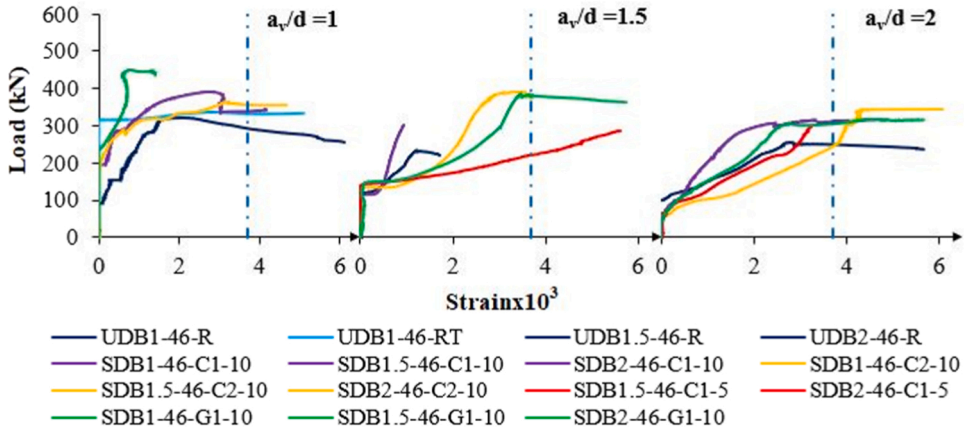

Fig. 7. : Load-strain curves obtained from the strain gauge "3".

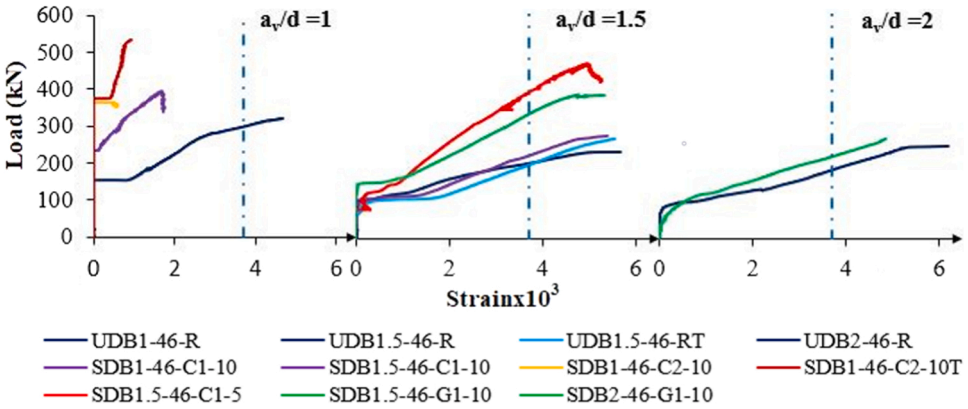

Fig. 8. : Load-strain curves obtained from the strain gauge "4".

parameters such as concrete strength, a_v/d, failure mode of beam, FRP strengthening scheme (S, U, W), effective strain in FRP strips, bond between FRP and concrete, anchorage length, shear crack angle and workmanship defect. It is not easy to develop a shear model considering the influence of all parameters. Therefore, researchers have taken into account only the parameters that they consider important in terms of the shear behavior of RC deep beams while developing their models.

The most significant parameter in the considered models is the effective strain or stress in the FRP strips. Triantafillou and

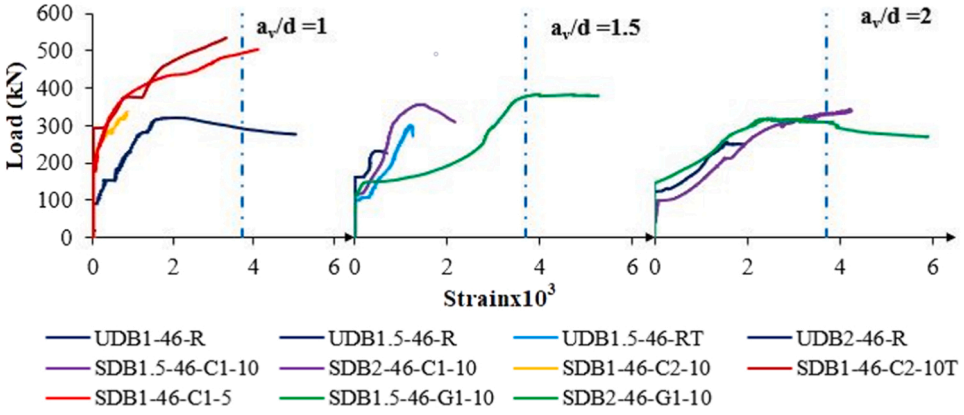

Fig. 9. : Load-strain curves obtained from the strain gauge "5".

Table 3
Prediction of the contribution of the FRP strips to the shear capacity of beams.

Guide Name	Summary of calculation steps
ACI 440 2R-17[60]	$V_f = A_{fv} f_{fe} (\sin\alpha + \cos\alpha) d_{fv}/s_f$; $A_{fv} = 2nt_f w_f$; $f_{fe} = \varepsilon_{fe} E_f$; $\varepsilon_{fe} = 0.004 \leq 0.75 C_E \varepsilon_{fu}$ $C_E = 0.85$
FIB-2001[61]	$V_f = 0.9 \varepsilon_{fk,e} E_f \rho_f b_w d(\cot\theta + \cot\alpha)\sin\alpha$; $\rho_f = (2nt_f w_f/s_f b_w)(strips)$; $\varepsilon_{fk,e} = k\varepsilon_{fe}$ $k = 0.8$: $\varepsilon_{fe} = 0.17(f_{cm}^{2/3}/E_f\rho_f)\varepsilon_{fu} \leq 0.006$
CNR-DT 200/2013[62]	$V_f = 0.9 d f_{fe} 2nt_f(\cot\theta + \cot\alpha) w_f/s_f$; $f_{fe} = f_{fd}[1 - \frac{1}{6}\frac{L_e \sin\alpha}{min(0.9d, h_w)}] + (\frac{1}{2}(k_R f_{fu} - f_{fd})[1 - \frac{1}{6}\frac{L_e \sin\alpha}{min(0.9d, h_w)}])$; $k_R = 0.2 + 1.6 r_c/b_w$ for $0 \leq r_c/b_w \leq 0.5$; $f_{fd} = \sqrt{(2E_f \Gamma_{rd})/(nt_f)}$; $\Gamma_{rd} = k_b k_G \sqrt{f_{cm} f_{ctm}}/FC$; $FC = 1$; $k_G = 0.037 mm$ $k_b = \left\{ \begin{array}{ll} \sqrt{\frac{2-(w_f/b_w)}{1+(w_f/b_w)}} & if \quad w_f/b_w \geq 0.25 \\ 1.18 & if \quad w_f/b_w < 0.25 \end{array} \right\}$; $L_e = \sqrt{\pi^2 s_u^2 E_f nt_f/(8\Gamma_{rd})}$; $s_u = 0.25 mm$
TR-55[63]	$V_f = 2nt_f w_f (d_{fv} - (n_{sc}/3) L_e \cos\alpha) E_f \varepsilon_{fe} (\sin\alpha + \cos\alpha)/s_f$; $n_{sc} = 0$ for fully wrapped $\varepsilon_{fe} = min\{\varepsilon_{fu}/2, \quad 0.5\sqrt{f_{ctm}/E_f nt_f}, \quad 0.004\}$; $L_e = 0.7\sqrt{E_f nt_f/f_{ctm}}$
German[64]	$V_f = 2nt_f w_f z f_{fe} \cot\theta/s_f$ $f_{fe} = k_R a_t f_{fu}$; $a_t = 1$; $k_R = \left\{ \begin{array}{ll} 0.5 r_c (2 - r_c/60)/60 & if \quad r_c < 60 \\ 0.5 & if \quad r_c \geq 60 \end{array} \right\}$
NCHRP Project No. 12–75 [65]	$V_f = A_{fv} f_{fe} d_{fv} (\cot\theta + \cot\alpha)\sin\alpha/s_f$; $f_{fe} = \varepsilon_{fe} E_f$; $\varepsilon_{fe} = R_f \varepsilon_{fu}$; $R = 4(\rho_f E_f)^{-0.67}$ for fully wrapped
CSA-S806–12[66]	$V_f = A_{fv} f_{fe} (\sin\alpha + \cos\alpha) d_{fv}/s_{fv}$; $A_{fv} = 2nt_f w_f$; $f_{fe} = \varepsilon_{fe} E_f$; $\varepsilon_{fe} = 0.006$ for fully wrapped
CIDAR[67]	$V_f = 2 f_{fe} t_f w_f h_{fe} (\cot\theta + \cot\alpha)\sin\alpha/s_f$; $h_{fe} = z_b - z_t$; $z_b = 0.9d - d_{fb}$; $z_t = d_{ft}$ $f_{fe} = D_f f_{fd,max}$; $D_f = 0.5(1 + z_t/z_b)$ $f_{fd,max} = \left\{ \begin{array}{ll} \phi_r f_{fu} & if \quad \varepsilon_f \leq 1.5\% \\ \phi_r \varepsilon_{fu} E_f & if \quad \varepsilon_f > 1.5\% \end{array} \right\}$; $\phi_r = 0.8$
Khalifa et al.[68]	$V_f = A_{fv} f_{fe} (\sin\alpha + \cos\alpha) d_{fv}/s_{fv}$; $f_{fe} = R f_{fu}$; $R = 0.5622(\rho_f E_f)^2 - 1.2188(\rho_f E_f) + 0.778 \leq 0.5$
Triantafillou and Antonopoulos[69]	
Chen and Teng[70] Kotynia[71]	$V_f = 2 f_{fe} t_f w_f h_{fe} (\cot\theta + \cot\alpha)\sin\alpha/s_f$; $f_{fe} = D_f f_{fu}$; $D_f = (1 + \zeta)/2$; $\zeta = z_t/z_b$; $h_{fe} = z_b - z_t$ $z_b = 0.9d$ and $z_t = 0$ for fully wrapped

Antonopoulos [69], Khalifa et al. [68] and NCHRP Project No. 12–75[65] proposed different effective strain expressions for the contribution of the FRP stirps to the shear strength based on a statistical analysis of a large database. The FRP type, debonding and the rupture conditions of the FRP strips were taken into account in these models. ACI 440.2R-17[60] proposes a shear model based on Khalifa et al. [68]'s model, while the FIB-2001[61] presents a model based on Triantafillou and Antonopoulos [69]'s model. The maximum effective strain in case of the beams fully wrapped with externally bonded FRP strips should be 0.004 according to ACI 440.2R-17[60] and TR-55[63. On the other hand, it is given as 0.006 in CSA-S806–12 [66]. CNR-DT200/2013[62] proposes a shear model based on fracture mechanics rather than statistical analysis. In addition, the physical limitation of a strengthened beam is tried to be considered in this code, where a coefficient regarding to the radius of rounded corners of beams in case of fully wrapping scheme

Table 4
Comparison of Experimental Results with Predictions.

Beam No	v_{fexp} MPa	v_{fe}/v_f, [60]	v_{fe}/v_f, [61]	v_{fe}/v_f, [62]	v_{fe}/v_f, [63]	v_{fe}/v_f, [64]	v_{fe}/v_f, [65]	v_{fe}/v_f, [66]	v_{fe}/v_f, [67]	v_{fe}/v_f, [68]	v_{fe}/v_f, [69]	v_{fe}/v_f, [70]	v_{fe}/v_f, [71]
SDB1–46-C1–10	0.66	0.40	0.30	0.87	0.57	0.31	1.32	0.27	0.26	0.25	0.36	0.21	0.20
SDB1.5–46-C1–10	0.78	0.47	0.35	1.03	0.67	0.37	1.55	0.31	0.30	0.29	0.42	0.24	0.24
SDB2–46-C1–10	1.16	0.70	0.52	1.53	1.00	0.55	2.31	0.47	0.45	0.44	0.63	0.36	0.36
SDB1–46-C2–10	0.38	0.11	0.11	0.32	0.23	0.09	0.60	0.08	0.15	0.17	0.10	0.12	0.06
SDB1–46-C2–10 T	2.74	0.83	0.76	2.28	1.66	0.65	4.33	0.55	1.07	1.24	0.74	0.85	0.42
SDB1.5–46-C2–10	1.25	0.38	0.35	1.04	0.76	0.30	1.98	0.25	0.49	0.56	0.34	0.39	0.19
SDB2–46-C2–10	1.28	0.39	0.35	1.06	0.77	0.30	2.01	0.26	0.50	0.58	0.34	0.40	0.20
SDB1–46-C1–5	2.66	1.07	0.91	2.34	1.52	0.84	4.62	0.72	0.69	1.04	0.96	0.55	0.55
SDB1.5–46-C1–5	2.26	0.91	0.77	1.99	1.29	0.71	3.93	0.61	0.59	0.89	0.81	0.47	0.47
SDB2–46-C1–5	1.32	0.53	0.45	1.16	0.75	0.42	2.29	0.35	0.34	0.52	0.47	0.27	0.27
SDB1–46-G1–10	1.48	3.18	2.36	4.20	3.18	0.86	1.54	2.12	0.71	0.51	2.83	0.57	0.56
SDB1.5–46-G1–10	1.15	2.46	1.83	3.26	2.46	0.66	1.20	1.64	0.55	0.39	2.19	0.44	0.43
SDB2–46-G1–10	0.84	1.80	1.33	2.38	1.80	0.49	0.87	1.20	0.40	0.29	1.60	0.32	0.32
Avarage		1.02	0.80	1.80	1.28	0.50	2.20	0.68	0.50	0.55	0.91	0.40	0.33
Std. Deviation		0.92	0.67	1.08	0.83	0.23	1.31	0.61	0.24	0.32	0.81	0.19	0.15
CoV		0.90	0.83	0.60	0.65	0.46	0.60	0.90	0.47	0.58	0.90	0.47	0.46

is given [62].

It can be seen in Table 4 the coefficient of variation (CoV) of the ratio of experimental result to the predicted contribution of the FRP strips ranges from 58% to 90%. These high values indicate that the results are not homogeneously distributed. It can be also seen in Table 4 that while the average values are conservative if the models of ACI 440.2R-17[60], CNR-DT200/2013[62], TR-55[63] and NCHRP Project No. 12–75[65] are used, it is nonconservative if the models of FIB-2001[61], CSA-S806–12 [66], Khalifa et al. [68] and Triantafillou and Antonopoulos [69] are used. It is suggested that the effective strain or stress expression in these models [60–63,65,66,68,69] should be revised according to a_v/d.

The main difference of the model proposed by Chen and Teng [70] from the others is the non-uniform stress distribution in the FRP along the shear crack, which is taken into account explicitly. CIDAR [67] gives equations for predicting the contribution of the FRP strips to the shear strength based on the model proposed by Chen and Teng [70]. The main difference of the model proposed by the German code [64] from the others is that the contribution of the FRP strips to the shear strength computed for beams fully wrapped with the FRP strips depends on the radius of rounded corners of beams. For the model proposed by Kotynia [71], the difference from the other models is the determination of the shear crack angle according to the transverse reinforcement ratio. Due to these significant differences, the coefficients of variation of the ratio of experimental result to the predicted contribution of the FRP strips by using these models [64,67,70,71] are 46–47% (Table 4). These coefficients are superior to the others in terms of homogeneity, but the average values are nonconservative. The model with the lowest coefficient of variation (46%) belongs to the German code [64] and Kotynia [71]. It can be inferred that the model proposed by the German code [64] is the one delivering the best predictions of the contribution of the FRP strips to the shear strength for the beams in this study, since the average value for the German code [64] (0.50) is closer to 1 than the average value for Kotynia [71] (0.33).

5. Conclusions

This study consists of two parts as the experimental study and the comparison of the experimental results with the predictions by various models. The following conclusions have been drawn.

1. The use of steel plates at the supports and loading point affected the shear behavior of the RC deep beams and the effectiveness of the FRP strips.

2. The rupture of the FRP strips is an indication for consuming the mechanical properties of FRP effectively. The rupture of the FRP strips occurred in all beams having an FRP strip spacing of 100 mm. However, it did not occur in the beams having an FRP strip spacing of 150 mm, except SDB1.5–46-C1–10. Therefore, it is recommended that the spacing of FRP strips should not exceed d/2.

3. As the a_v/d increased, the increase in the shear capacity of strengthened beams decreased, while it was the opposite for the deflection capacity.

4. Increasing the number of FRP layers by one, reducing the spacing of the FRP strips or using GFRP strips improved the shear and deflection capacities.

5. The use of GFRP instead of CFRP yielded higher increases in the shear and deflection capacities of the beam having an a_v/d of 1.5. However, for the beam having an a_v/d of 2, it was the opposite.

6. The changes in the first shear cracking loads of the strengthened beams were not significant compared to those of the unstrengthened beams for a given a_v/d. The angle of shear cracks in the tested beams ranged from 40° to 60°. However, the shear crack angle decreased until 26° in beams having a_v/d of 2.

7. Unstrengthened beams exhibited nonductile behavior. The behavior of strengthened beams having a_v/d ratios of 1 and 1.5 was also nonductile, but the behavior of strengthened beams with an a_v/d ratio of 2 was ductile.

8. The most significant parameters affecting the strains were the a_v/d and the type of FRP.

9. The comparison of the experimental results with the predictions obtained from the models consisting of those given by various codes [60–67] and those proposed by various researchers [68–71] resulted in coefficients of variation varying between 58% and 90%, which indicates that the results are not homogeneously distributed. It is suggested that the effective strain or stress expression in these models [60–63,65,66,68,69] should be revised according to a_v/d.

10. The comparison of the experimental results with the predictions obtained from the models [64,67,70,71] resulted in coefficients of variation equal to 46–47%, which are superior to the other in terms of homogeneity. The model proposed by German code [64] delivered the best predictions of the contribution of the FRP strips to the shear strength for the beams in this study.

Declaration of Competing Interest

The authors declare the following financial interests/personal relationships which may be considered as potential competing interests: Hasan Cem AKKAYA reports financial support was provided by Yildiz Technical University.

Acknowledgment

This work was supported by Research Fund of the Yildiz Technical University, Turkey Project Number: FDK-2021–4804.

References

[1] A. Demir, N. Caglar, H. Ozturk, Parameters affecting diagonal cracking behavior of reinforced concrete deep beams, Eng. Struct. 184 (2019) 217–231.
[2] ACI Committee 318 (2019). Building Code Requirements for Structural Concrete (ACI 318–19) and Commentary (ACI 318R-19). American Concrete Institute, Farmington Hills, MI, 623 pp.
[3] EN 1992–1-1, Eurocode 2: design of concrete structures. General rules and rules for buildings. 3, 2004.
[4] A.H. Nilson, D. Darwin, Design of Concrete Structures. McGraw-Hill International Editions, 1997. 12th Edition.
[5] G. Russo, R. Venir, M. Pauletta, Reinforced concrete deep beams-shear strength model and design formula, Acids Struct. J. 102 (3) (2005) 429.
[6] G.A. Rao, K. Kunal, R. Eligehausen, Shear strength of RC deep beams. In Proceedings of the 6th International Conference on Fracture Mechanics of Concrete and Concrete Structures (2007, June), Catania (pp. 693–699).
[7] B. Mohammed, B.H. Bakar, K. Choong, The effects of opening on the structural behavior of masonry wall subjected to compressive loading—strain variation, Open Civ. Eng. J. 3 (2009) 62–73.
[8] N.I. Rahim, B.S. Mohammed, A. Al-Fakih, M.M.A. Wahab, M.S. Liew, A. Anwar, Y.H. Amran, Strengthening the structural behavior of web openings in RC deep beam using CFRP, Materials 13 (12) (2020) 2804.
[9] M. Mahmod, A.N. Hanoon, H.J. Abed, Flexural behavior of self-compacting concrete beams strengthened with steel fiber reinforcement, J. Build. Eng. 16 (2018) 228–237.
[10] A.H.A. Zaher, W.M. Montaser, M.M. Elsonbaty, Strengthening and Repairing of RC Deep Beams Using CFRP and GFRP, Int. J. Civ. Eng. Technol. 11 (2020) 1.
[11] A. Belarbi, B. Acun, FRP systems in shear strengthening of reinforced concrete structures, Procedia Eng. 57 (2013) 2–8.
[12] J.G. Teng, J.F. Chen, S.T. Smith, L. Lam, Behaviour and strength of FRP-strengthened RC structures: a state-of-the-art review, Proc. Inst. Civ. Eng. -Struct. Build. 156 (1) (2003) 51–62.
[13] A. Saribiyik, B. Abodan, M.T. Balci, Experimental study on shear strengthening of RC beams with basalt FRP strips using different wrapping methods, Eng. Sci. Technol., Int. J. 24 (1) (2021) 192–204.
[14] A.S. Farghaly, B. Benmokrane, Shear behavior of FRP-reinforced concrete deep beams without web reinforcement, J. Compos. Constr. 17 (6) (2013) 04013015.
[15] A.E. Ahmed, F.E. El-Salakawy, B. Benmokrane, Shear performance of RC bridge girders reinforced with carbon FRP stirrups, J. Bridge Eng. 15 (1) (2010) 44–54.
[16] (J.S.C.E.) Japan Society of Civil Engineers, Recommendation for design and construction of concrete structures using continuous fiber reinforcing materials, Concr. Eng. Ser. (1997) 23.
[17] O. Chaallal, A. Mofidi, B. Benmokrane, K. Neale, Embedded through-section FRP rod method for shear strengthening of RC beams: Performance and comparison with existing techniques, J. Compos. Constr. 15 (3) (2011) 374–383.
[18] K. Yang, H. Wang, Z. Liu, Evaluation on mechanical properties of high-performance biocomposite bridge deck structure: a review, Polym. Compos. 42 (12) (2021) 6265–6297.
[19] K. Sogut, S. Dirar, M. Theofanous, A. Faramarzi, A.N. Nayak, Effect of transverse and longitudinal reinforcement ratios on the behaviour of RC T-beams shear-strengthened with embedded FRP BARS, Compos. Struct. 262 (2021), 113622.
[20] Y.M. Saeed, W.A. Aules, F.N. Rad, A.M. Raad, Tensile behavior of FRP anchors made from CFRP ropes epoxy-bonded to uncracked concrete for flexural strengthening of RC columns. Case Studies in Construction, Materials 13 (2020), e00435.
[21] Y.Z. Murad, Retrofitting interior RC beam-to-column joints subjected to quasi-static loading using NSM CFRP ropes. In Structures (2021, December), Vol. 34, pp. 4158–4168. Elsevier.
[22] C.E. Chalioris, P.M.K. Kosmidou, N.A. Papadopoulos, Investigation of a new strengthening technique for RC deep beams using carbon FRP ropes as transverse reinforcements, Fibers 6 (3) (2018) 52.
[23] E. Golias, A.G. Zapris, V.K. Kytinou, G.I. Kalogeropoulos, C.E. Chalioris, C.G. Karayannis, Effectiveness of the novel rehabilitation method of seismically damaged RC joints using C-FRP ropes and comparison with widely applied method using C-FRP sheets—Experimental investigation, Sustainability 13 (11) (2021) 6454.
[24] C.E. Chalioris, V.K. Kytinou, M.E. Voutetaki, N.A. Papadopoulos, Repair of heavily damaged RC beams failing in shear using U-shaped mortar jackets, Buildings 9 (6) (2019) 146.

[25] C.E. Chalioris, A.G. Zapris, C.G. Karayannis, U-jacketing applications of fiber-reinforced polymers in reinforced concrete T-beams against shear—Tests and design, Fibers 8 (2) (2020) 13.
[26] H.H. Mhanna, R.A. Hawileh, J.A. Abdalla, Shear strengthening of reinforced concrete beams using CFRP wraps, Procedia Struct. Integr. 17 (2019) 214–221.
[27] A. Godat, Z. Qu, X.Z. Lu, P. Labossiere, L.P. Ye, K.W. Neale, Size effects for reinforced concrete beams strengthened in shear with CFRP strips, J. Compos. Constr. 14 (3) (2010) 260–271.
[28] J. Dong, Q. Wang, Z. Guan, Structural behaviour of RC beams with external flexural and flexural shear strengthening by FRP sheets, Compos Part B Eng. 44 (1) (2013) 604–612.
[29] A. Khalifa, A. Nanni, Rehabilitation of rectangular supported RC beams with deficiencies using CFRP composites, Constr. Build. Mater. 16 (3) (2002) 135–146.
[30] M.M. Rasheed, Retrofit of reinforced concrete deep beams with different shear reinforcement by using CFRP, Civil Environ. Res. 8 (2016) 5.
[31] A. Li, C. Diagana, Y. Delmas, CRFP contribution to shear capacity of strengthened RC beams, Eng. Struct. 23 (10) (2001) 1212–1220.
[32] A.K. Panigrahi, K.C. Biswal, M.R. Barik, Strengthening of shear deficient RC T-beams with externally bonded GFRP sheets, Constr. Build. Mater. 57 (2014) 81–91.
[33] J. Sim, G. Kim, C. Park, M. Ju, Shear strengthening effects with varying types of FRP materials and strengthening methods. In 7th International Symposium on Fiber-Reinforced Polymer (FRP) Reinforcement for Concrete Structures (2005, October), pp. 1665–1680.
[34] K. Uji, Improving shear capacity of existing reinforced concrete members by applying carbon fiber sheets, Trans. Jpn. Concr. Inst. 14 (1992) 253–266.
[35] M.J. Chajes, T.F. Januszka, D.R. Mertz, T.A. Thomson, W.W. Finch, Shear strengthening of reinforced concrete beams using externally applied composite fabrics, Struct. J. 92 (3) (1995) 295–303.
[36] O. Chaallal, M.J. Nollet, D. Perraton, Shear strengthening of RC beams by externally bonded side CFRP strips, J. Compos. Constr. 2 (2) (1998) 111–113.
[37] B. Täljsten, L. Elfgren, Strengthening concrete beams for shear using CFRP-materials: evaluation of different application methods, Compos. Part B: Eng. 31 (2) (2000) 87–96.
[38] C. Diagana, A. Li, B. Gedalia, Y. Delmas, Shear strengthening effectiveness with CFF strips, Eng. Struct. 25 (4) (2003) 507–516.
[39] B.B. Adhikary, H. Mutsuyoshi, Behavior of concrete beams strengthened in shear with carbon-fiber sheets, J. Compos. Constr. 8 (3) (2004) 258–264.
[40] A.S. Mosallam, S. Banerjee, Shear enhancement of reinforced concrete beams strengthened with FRP composite laminates, Compos. Part B: Eng. 38 (5–6) (2007) 781–793.
[41] Y. Zhou, M. Gou, F. Zhang, S. Zhang, D. Wang, Reinforced concrete beams strengthened with carbon fiber reinforced polymer by friction hybrid bond technique: Experimental investigation, Mater. Des. 50 (2013) 130–139.
[42] R.A. Hawileh, H.A. Rasheed, J.A. Abdalla, A.K. Al-Tamimi, Behavior of reinforced concrete beams strengthened with externally bonded hybrid fiber reinforced polymer systems, Mater. Des. 53 (2014) 972–982.
[43] T. Skuturna, J. Valivonis, Design method for calculating load-carrying capacity of reinforced concrete beams strengthened with external FRP, Constr. Build. Mater. 50 (2014) 577–583.
[44] A.K. El-Sayed, Effect of longitudinal CFRP strengthening on the shear resistance of reinforced concrete beams, Compos. Part B: Eng. 58 (2014) 422–429.
[45] E. Grande, M. Imbimbo, A. Rasulo, Effect of transverse steel on the response of RC beams strengthened in shear by FRP: Experimental study, J. Compos. Constr. 13 (5) (2009) 405–414.
[46] A.S. Karzad, M. Leblouba, S. Al Toubat, M. Maalej, Repair and strengthening of shear-deficient reinforced concrete beams using Carbon Fiber Reinforced Polymer, Compos. Struct. 223 (2019), 110963.
[47] ACI (American Concrete Institute) (2008). Guide for the design and construction of externally bonded FRP systems for strengthening concrete structures. ACI Committee 440, Farmington Hills, MI.
[48] Z. Zhang, C.T.T. Hsu, J. Moren, Shear strengthening of reinforced concrete deep beams using carbon fiber reinforced polymer laminates, J. Compos. Constr. 8 (5) (2004) 403–414.
[49] M.R. Islam, M.A. Mansur, M. Maalej, Shear strengthening of RC deep beams using externally bonded FRP systems, Cem. Concr. Compos. 27 (3) (2005) 413–420.
[50] H.K. Lee, S.H. Cheong, S.K. Ha, C.G. Lee, Behavior and performance of RC T-section deep beams externally strengthened in shear with CFRP sheets, Compos. Struct. 93 (2) (2011) 911–922.
[51] M.A. Javed, M. Irfan, S. Khalid, Y. Chen, S. Ahmed, An experimental study on the shear strengthening of reinforced concrete deep beams with carbon fiber reinforced polymers, KSCE J. Civ. Eng. 20 (7) (2016) 2802–2810.
[52] A. Bousselham, O. Chaallal, Behavior of reinforced concrete T-beams strengthened in shear with carbon fiber-reinforced polymer-an experimental study, Acids Struct. J. 103 (3) (2006) 339.
[53] ACI Committee 440, 2002, Design and Construction of Externally Bonded FRP Systems for Strengthening Concrete Structures (440.2R-02). American Concrete Institute, Farmington Hills, Mich.
[54] Canadian Standards Association, 2002, Design and Construction of Building Components with Fiber-Reinforced Polymer, CSA-S806–02,.Rexdale, Ontario, Canada.
[55] W. Li, C.K. Leung, Shear span–depth ratio effect on behavior of RC beam shear strengthened with full-wrapping FRP strip, J. Compos. Constr. 20 (3) (2016) 04015067.
[56] Japan Society of Civil Engineers (JSCE). Recommendations for upgrading of concrete structures with use of continuous fiber sheets. 2001, Japan.
[57] W. Li, C.K. Leung, Effect of shear span-depth ratio on mechanical performance of RC beams strengthened in shear with U-wrapping FRP strips, Compos. Struct. 177 (2017) 141–157.
[58] S.Y. Cao, J.F. Chen, J.G. Teng, Z. Hao, J. Chen, Debonding in RC beams shear strengthened with complete FRP wraps, J. Compos. Constr. 9 (5) (2005) 417–428.
[59] A. Kumari, A.N. Nayak, Strengthening of shear deficient RC deep beams using GFRP sheets and mechanical anchors, Can. J. Civ. Eng. 48 (1) (2021) 1–15.
[60] ACI Committee 440, Guide for the Design and Construction of Externally Bonded FRP Systems for Strengthening Concrete Structures (ACI 440.2R-17). Farmington Hills, MI: American Concrete Institute, 2017.
[61] Fédération Internationale du Béton (fib), Externally bonded FRP reinforcement for RC structures. Task Group 9.3, Bullettin No. 14, Lausanne, Switzerland, 201.
[62] CNR-Italian Research Council, Advisory Committee on Technical Recommendations for Construction, 2013, Guide for the Design and Construction of Externally Bonded FRP Systems for Strengthening Existing Structures. Materials, RC and PC Structures, Masonry Structures (CNR-DT 200/2013). Rome, Italy.
[63] Concrete Society: Design guidance for strengthening concrete structures using fibre composite materials, TR 55, 2012, Crowthorne, UK.
[64] German Committee for Structural Concrete: Strengthening of concrete members with adhesively bonded reinforcement. DAfStb, 2012, German.
[65] A. Belarbi, S.-W. Bae, A. Ayoub, D. Kuchma, A. Mirmiran, A.M. Okeil, Design of FRP systems for strengthening concrete girders in shear. NCHRP Rep. No. 678 (2011), Transportation Research Board, Washington, DC.
[66] CSA-S806–12 (2012) Design and construction of building components with fibre-reinforced polymers. Canadian Standards Association, Mississauga.
[67] CIDAR, Design Guideline for RC structures retrofitted with FRP and metal plates: beams and slabs. Draft 3 - Submitted ToStandards Australia, The University of Adelaide, 206.
[68] A. Khalifa, W.J. Gold, A. Nanni, A.A. MI, Contribution of externally bonded FRP to shear capacity of RC flexural members, J. Compos. Constr. 2 (4) (1998) 195–202.
[69] T.C. Triantafillou, C.P. Antonopoulos, Design of concrete flexural members strengthened in shear with FRP, J. Compos. Constr. 4 (4) (2000) 198–205.
[70] J.F. Chen, J.G. Teng, Shear capacity of fiber-reinforced polymer-strengthened reinforced concrete beams: Fiber reinforced polymer rupture, J. Struct. Eng. 129 (5) (2003) 615–625.
[71] R. Kotynia, Shear strengthening of RC beams with polymer composites. Associate Professor Thesis, Łódź, 2011.